University of Alberta

Flow Pattern Effects on Aerosol Size Distributions of Dry Powder Inhalers

by

Michael Grant Gehmlich ©

A thesis submitted to the Faculty of Graduate Studies and Research in partial fulfillment of the requirements for the degree of Master of Science.

Department of Mechanical Engineering

Edmonton, Alberta

Spring 2000

National Library of Canada
Acquisitions and Bibliographic Services
395 Wellington Street
Ottawa ON K1A 0N4
Canada

Bibliothèque nationale du Canada
Acquisitions et services bibliographiques
395, rue Wellington
Ottawa ON K1A 0N4
Canada

Your file Votre référence

Our file Notre référence

The author has granted a non-exclusive licence allowing the National Library of Canada to reproduce, loan, distribute or sell copies of this thesis in microform, paper or electronic formats.

L'auteur a accordé une licence non exclusive permettant à la Bibliothèque nationale du Canada de reproduire, prêter, distribuer ou vendre des copies de cette thèse sous la forme de microfiche/film, de reproduction sur papier ou sur format électronique.

The author retains ownership of the copyright in this thesis. Neither the thesis nor substantial extracts from it may be printed or otherwise reproduced without the author's permission.

L'auteur conserve la propriété du droit d'auteur qui protège cette thèse. Ni la thèse ni des extraits substantiels de celle-ci ne doivent être imprimés ou autrement reproduits sans son autorisation.

0-612-60122-6

Canada

University of Alberta

Library Release Form

Name of Author: Michael Grant Gehmlich

Title of Thesis: Flow Pattern Effects on Aerosol Size Distributions of Dry Powder Inhalers

Degree: Master of Science

Year this Degree Granted: 2000

Permission is hereby granted to the University of Alberta to reproduce single copies of this thesis and to lend or sell such copies for private, scholarly or scientific research purposes only.

The author reserves all other publication and other rights in association with the copyright in the thesis, and except as herein before provided , neither the thesis nor any substantial portion thereof may be printed or otherwise reproduced in any material form whatever without the author's prior written permission.

Michael G Gehmlich

10209 – 79 Street
Edmonton, Alberta
T6A 3G6

09 November 1999

University of Alberta

Faculty of Graduate Studies and Research

The undersigned certify that they have read , and recommend to the Faculty of Graduate Studies and Research for acceptance, a thesis entitled "Flow Pattern Effects on Aerosol Size Distributions of Dry Powder Inhalers" submitted by Michael Grant Gehmlich in partial fulfillment of the requirements for the degree of Master of Science.

Dr. Warren H. Finlay

Dr. Dongqing Li

Dr. Krishnaswamy Nandakumar

03 November 1999

Abstract

Currently accepted methods for *in vitro* testing of dry powder inhalers prescribe that the flow through the inhaler is maintained at a constant rate during testing. This does not closely resemble the actual flow through the device when used by a patient. Studies have shown that the flow rate through a dry powder inhaler affects the size distribution of the drug aerosol produced.

This body of work introduces an apparatus and method of testing dry powder inhalers that allows *in vitro* testing with realistic flow patterns. Aerosol size distributions produced with realistic breathing patterns are compared to distributions produced with constant flow rates.

This work concludes that for the Spiros and Ventodisk inhalers, constant flow rate testing is an acceptable alternative to testing with realistic flow patterns provided the flow rate used resembles the average flow rate expected during actual patient use.

Acknowledgements

The laboratory and technical help of H. Orszanska, C. Shute, B. Faulkner, B.Hennig, T. Gear, the medical help and patients of Dr. P. Zuberbuler, the financial support of the Alberta Lung Association and the Natural Science and Engineering Research Council and the supervision and patience of Dr. W. Finlay, is gratefully acknowledged.

Table Of Contents

1. Introduction 1

2. Current Testing Methods and Devices 3

2.1. Introduction 3

2.2. Devices 3

2.2.1. Cascade Impactor 4

2.2.2. USP Induction Port 5

2.3. Pharmacopeial Procedures 5

2.4. Size Determination 6

3. Design Presentation and Procedure 10

3.1. Introduction 10

3.2. Apparatus Description 10

3.2.1. MOUDI Impactor 11

3.2.2. Virtual Impactor 11

3.2.3. Mouth and Throat 12

3.2.4. Happy Breathing Machine 12

3.2.5. Inhaler Enclosure 12

3.2.6. Makeup Airflow Entrainment Tube 13

3.3. Setup and Procedures 13

3.4. Size Determination 14

4. Validation 20

4.1. Introduction 20

4.2. Analytical Validation 20

4.3. Experimental Validation 24

4.3.1. Ventodisk 25

4.3.2. Spiros 26

4.3.3. Turbuhaler 26

5. Plethysmograph and Breathing Data 32
5.1. Introduction 32
5.2. Plethysmograph 32
5.2.1. Apparatus Description 32
5.2.2. Operational Procedure 33
5.3. Breath Patterns 34

6. Tests and Results 38
6.1. Introduction 38
6.2. Flow Pattern Comparative Tests 38
6.3. Test Results 39
6.3.1. Ventodisk 39
6.3.2. Spiros 41

7. Conclusions and Future Work 47

8. References 49

List of Tables

Table 4.1. Values of parameters. 23
Table 4.2. Ratios of particle force for each MOUDI impactor stage and virtual impactor stage. 23
Table 4.3. Critical Diameter of an agglomerated drug particle for deaggregation to occur as a result of acceleration forces in turbulent eddies. 24

Table 5.1. Distributions of age and gender among the volunteers involved in the breath pattern survey. 34

Table 6.1. Listing of the flow rates and breathing patterns to be compared in each device including the volume of each set of compared flows. 39
Table 6.2. MMADs and GSDs for the 5-run grouped test data. 40

List of Figures

Figure 2.1. Impactor stage 7
Figure 2.2. Impactor collection efficiency curve 7
Figure 2.3. Cascade Impactor 8
Figure 2.4. USP Induction port cross-sectional view 9

Figure 3.1. Virtual impactor stage 16
Figure 3.2. Flow diagram of the CAVIC 17
Figure 3.3. Realistic mouth and throat assembly 18
Figure 3.4. Upper CAVIC assembly diagram 19

Figure 4.1. Size distributions measured by the MOUDI and CAVIC impactors for validation of the Ventodisk inhaler. 28
Figure 4.2. Size distributions to check for overloading for validation of the Ventodisk inhaler. 29
Figure 4.3. Size distributions measured by the MOUDI and CAVIC impactors for validation of the Spiros inhaler. 30
Figure 4.4. Size distributions measured by the MOUDI and CAVIC impactors for validation of the Turbuhaler inhaler. 31

Figure 5.1. Schematic of the Plethysmograph. 35
Figure 5.2. Breathing patterns that were generated and used with the Ventodisk dry powder inhaler. 36
Figure 5.3. Breathing patterns that were generated and used with the Spiros dry powder inhaler. 37

Figure 6.1. Size distributions of the slow breathing pattern tests for the Ventodisk inhaler. 43
Figure 6.2. Size distributions of the fast breathing pattern tests for the Ventodisk inhaler. 44
Figure 6.3. Size distributions of the slow breathing pattern tests for the Spiros inhaler. 45
Figure 6.4. Size distributions of the fast breathing pattern tests for the Spiros inhaler. 46

1. Introduction

An aerosol is a suspension of liquid or solid particles in air. Aerosols exist naturally in the earth's atmosphere. Some examples are dust, pollen (solid particles) and fog (liquid particles). Other aerosols are man-made and are produced by industry. Some examples are spray air-fresheners or cooling processes in manufacturing.

Regardless of the origin of the aerosol, airborne particles are inhaled during the normal breathing cycle. Inhaled particles may deposit in the nasal cavity, throat or lungs or may not deposit at all and be exhaled back into the atmosphere. A particles deposition site is affected by many factors including particle size, air flow rate and lung morphology. While much of the deposited aerosol is removed by the body's natural defense system, having little effect, some particles may cause adverse effects such as pollen causing an allergic reaction. Deposition of aerosol particles can also have positive effects. By targeting the size of particles that the body is least capable of removing, medical science uses inhaled aerosols to deliver drugs to the lung to treat pulmonary disorders such as asthma or cystic fibrosis.

There are three common types of devices used to produce medical aerosols. The nebulizer produces aerosols from drug solutions or suspensions using air-water spray atomization technology. Nebulizers are used most commonly by hospitals and young children and require a source of compressed air or a portable compressor. Metered dose inhalers use a pressurized canister to produce a precisely measured volume of inhalable spray. The canister contains a formulation of solution or suspension of active drug in propellant. While inexpensive and convenient, metered dose inhalers can be completely ineffectual if not used properly. Dry powder inhalers contain finely milled drug powder that often require inhalation power to deaggregate the powder. Expense and convenience are similar to the metered dose inhaler, but many dry powder inhalers produce varying doses depending upon the inhalation flow rate and therefore have inconsistent results. This

variance in dosage stems from agglomeration of the milled drug particles while stored in bulk. The rate of airflow through the inhaler produces turbulence that deaggregates the particle agglomerates. Generally, higher flow rates produce more deaggregation and result in smaller particle size. Some newer dry powder inhalers use mechanisms to deaggregate the powder that do not rely on inhalation flow rate.

In order to improve the efficacy of therapeutic drug delivery, ongoing work is done in the scientific community to develop new and better inhalers. One of the easiest methods of testing the performance of an inhaler is by collection and measurement of the produced aerosol. This *in vitro* testing method gives a good measure of the inhalers consistency and can be used to estimate lung deposition of the drug.

This document focuses on dry powder inhalers and specifically the way these devices are tested. Typically, inhalers are tested with a flow rate through the device that is determined by the requirements of the aerosol collection equipment. This flow rate is constant and does not resemble a realistic inhalation flow pattern. The objective of the work detailed in this document is to determine how the difference in flow patterns through the tested device affects the characteristics of the aerosol being produced. These results will help determine if the current testing methods are adequate or if revisions should be made.

2. Current Testing Methods and Devices

2.1. Introduction

The currently accepted standardized testing methods for inhalers are described by the United States Pharmacopeia (USP). The USP includes descriptions and monographs on dosage forms for over 1000 drugs as well as information such as chemical and physical tests. For physical tests of aerosol drugs, it outlines the testing equipment to use and the procedure to follow. While the USP may present the officially accepted testing methods, many different methods and types of equipment are used for various reasons such as convenience or improved technique. Despite the numerous testing methods in use, only the USP methods and procedures are presented here. The USP also includes three apparatus options for aerosol testing but only the option with the greatest resolution for determining aerosol size is presented.

2.2. Devices

The main components involved in aerosol measurement are the cascade impactor, the induction port and the vacuum pump. The cascade impactor is the device that collects and measures the size of the aerosol particles. This is done by separating the aerosol into a number of different size ranges and then measuring the amount of drug in each size range. The induction port is simply a tube that makes a 90-degree bend. This device serves to simulate the mouth and throat of the person using the device as well as turn the airflow vertically to accommodate the cascade impactor. The vacuum pump powers the airflow through the cascade impactor. It functions at a calibrated flow rate that remains constant.

2.2.1. Cascade Impactor

A cascade impactor is simply a series of individual impactor stages with each progressive stage designed to measure a smaller sized particle. Each impactor stage consists of a nozzle or set of nozzles and an impaction plate as shown in Figure 2.1. The incoming particle laden flow is accelerated through the nozzles towards the impaction plate. The larger particles will impact on the plate and be removed from the flow while the smaller particles will travel with the flow around the plate. Whether or not a given particle will impact on the plate is determined by the particles Stokes number (c.f. Willeke & Baron), Stk, defined as

$$Stk = \frac{U_0 \cdot p_{part} \cdot (d_{part})^2 \cdot Cc}{18 \cdot \mu \cdot D} \tag{2.1}$$

where

U_0 = average fluid velocity in the nozzle;
p_{part} = particle density;
d_{part} = particle diameter;
Cc = Cunningham Slip Correction;
μ = dynamic viscosity of air;
D = nozzle diameter.

This equation assumes the particles are spherical, the Reynolds number of the particle is much less than 1, and particle density is much larger than the density of air. Stk is a dimensionless parameter defined as the ratio of the particles stopping distance to a characteristic dimension of the nozzle, in this case the nozzle diameter. If a particle's Stk is larger than about unity, then it will impact on the plate. Stk is also used to determine the cut-size of a particular impactor stage. The cut-size of the stage is the diameter of the particle that is collected with 50% efficiency.

An impactor's most important characteristic is its collection efficiency curve, as illustrated in Figure 2.2. The collection efficiency is the fraction of particles passing through the impactor nozzle that are collected on the impaction plate. A perfect impactor would have a straight vertical efficiency curve. This would mean that all particles larger than the impactors cut-size would impact on the plate and all particles smaller than the cut-size would follow the flow through.

The cascade impactor stacks a number of impactors in series so that the flow through one impactor would go straight into the next impactor with a slightly smaller cut-size as illustrated in Figure 2.3. The last stage of a cascade impactor is a filter that collects any remaining drug particles from the flow. This effectively separates the aerosol into 5 to 10 (depending on the number of stages) groups of particles with known size ranges.

The cascade impactor recommended by the USP is the Anderson MkII (Graseby-Anderson Inc., Atlanta, GA, USA). It is a multi-stage impactor with an end filter and an optional pre-separator filter. The pre-separator removes any particles over about 20μm and precedes the first impaction stage. The stages cut-sizes range from 10μm to 1μm and the impactor operates at a flow rate of 28.3 liters/min (1 cubic foot/min).

2.2.2. USP Induction Port

The induction port is what links the horizontally actuated inhaler to the vertical inlet of the cascade impactor. Other than providing for a change in flow direction, the induction port also provides for a certain amount of deposition at the corner of the bend. This deposition roughly simulates the deposition that would occur in a patients mouth and throat.

The induction port is made of aluminum or stainless steel and is built to strict dimensions. A representative diagram of the port is given in Figure 2.4 but is not drawn to scale for simplicity.

2.3. Pharmacopeial Procedures

A highly simplified set of procedures is presented in the following paragraph to outline the general testing method. For complete testing procedures please refer to United States Pharmacopeia revision 23 (1995).

For dry powder inhalers, modify the impaction plate of each stage to ensure that an impacted particle is not re-entrained into the flowing airstream by coating the collection surface with silicon fluid or other substance. Assemble the cascade impactor and pre-separator and attach the induction port. Attach the vacuum pump and calibrate the flow rate. Weigh the inhaler. With the pump running, prime or load the inhaler and insert it into the induction port. Leave the inhaler in place for 20 seconds to enable it to empty. If additional doses are required for the sample, repeat the loading and discharge procedure. Wash with solvent and dilute to an appropriate volume the inhaler mouthpiece, induction port, and all the impactor stages and end filter. Dry and weigh the inhaler to determine the amount of drug dispensed. Determine the mass of drug in each component by using the specified method from the drug monograph. Determination of drug mass is normally done with a UV spectrophotometer or by chromatography.

2.4. Size Determination

Aerosols that contain particles that are all the same size are called monodisperse aerosols. Monodisperse aerosols almost never exist naturally and are difficult to produce. An aerosol that contains particles of various sizes is called polydisperse. The distribution of a polydisperse aerosol typically follows a lognormal distribution.

The distribution of an aerosol is most commonly characterized by its median size. In particular, the mass median diameter is the diameter such that ½ of the mass of the aerosol particles is contained in particles with larger diameter and ½ the mass is contained in particles with smaller diameter. The amount of size variation is characterized by the geometric standard deviation (GSD).

For particles with diameter much greater than the mean free path of air (i.e. Cc=1), equation (2.1) shows that the only particle property that affects a particle's trajectory is its aerodynamic diameter, d_{ae}, defined as

$$d_{ae} = \sqrt{\rho_{part}} \cdot d_{part}. \tag{2.2}$$

Therefore, particles measured with an impactor measure aerodynamic diameter, and a distribution's characteristic size is the mass-median aerodynamic diameter (MMAD).

To determine the MMAD of an aerosol measured with a cascade impactor the drug mass data for each stage and the end filter are needed. The total drug mass collected in the impactor is calculated and the percentage of the total mass of each stage is determined. This data is used to create a "Cumulative Percent Found Less Than Stated Particle Size" graph. The procedure for creating such a plot is as follows: Start with the stage that captures the smallest sized particles (i.e. the end filter) and plot on log probability paper the percentage of mass on that stage versus the particle size (i.e. effective cut-size of the stage above it in the impactor). Do this for the remaining stages in ascending order, but add to each stage's percentage the total percentage found on all the stages below it. Draw the straight-line best fit or use a weighted least squares regression. The MMAD is the particle size at which the best-fit line crosses the 50% mark. For this reason the MMAD is often denoted by d_{50}.

The GSD is obtained from the same graph as the MMAD. Note the particle size at which the line crosses the 84.13% mark, d_{84}, and the 15.87% mark, d_{15}. The GSD is calculated from equation (2.3). An aerosol with a log-normal distribution can be

$$GSD = \sqrt{\frac{d_{84}}{d_{15}}} \tag{2.3}$$

totally characterized by its MMAD and GSD.

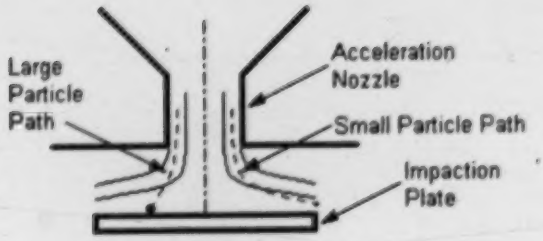

Figure 2.1. Impactor Stage

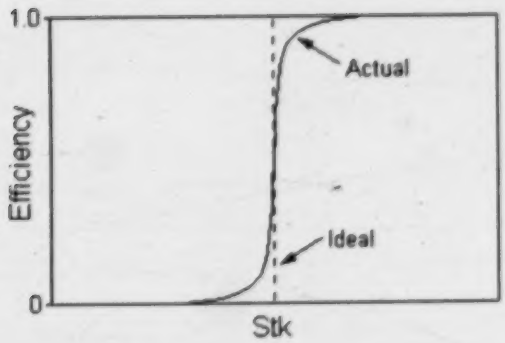

Figure 2.2. Impactor Collection Efficiency Curve

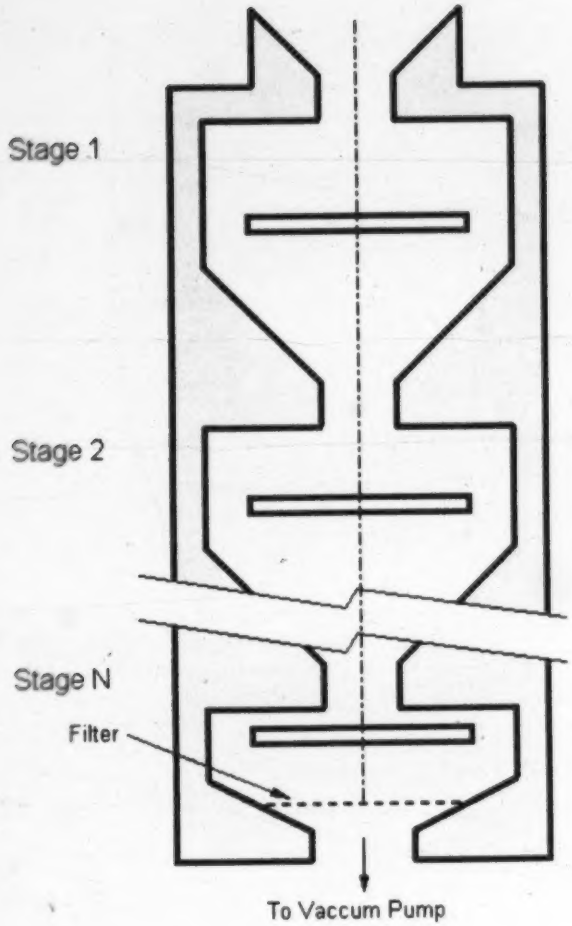

Figure 2.3. Cascade Impactor

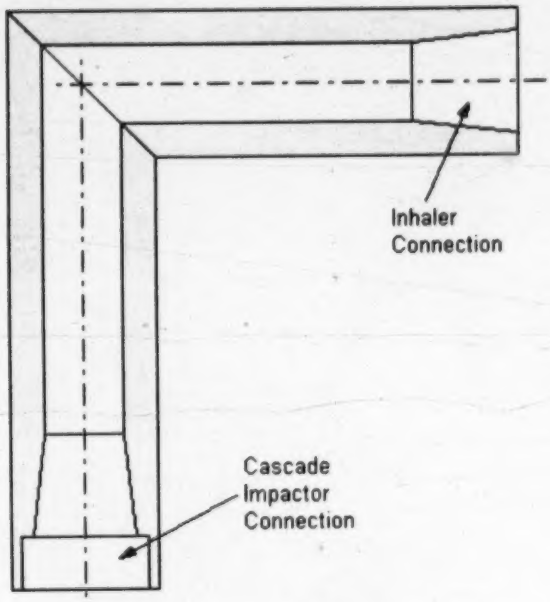

Figure 2.4. USP Induction Port cross-sectional view

3. Design Presentation and Procedure

3.1. Introduction

The methods and equipment used in this study vary significantly from those outlined in the USP. The principal reason for this has a functional basis. In particular, for the effects of realistic breathing patterns on generated aerosol size to be studied, it is required that the inhaler be sampled at variable flow rates, which is not possible with the USP setup. The most significant feature of the presented design is the capability to generate and test an inhaler with any flow rate or flow pattern. This is accomplished with several unique components. The major elements of the design that will be discussed further are a cascade impactor, a virtual impactor, a realistic mouth and throat and a breathing simulation machine. Since the presented apparatus uses a Cascade And Virtual Impactor Combination it is referred to as the CAVIC.

The principal requirement of this presented design is that of non-intrusive testing. This means that the CAVIC must be able to collect the generated aerosol without altering the characteristics or physical properties of the aerosol and without excessive aerosol losses. These requirements were focused on during design and selection of the various components of the CAVIC.

3.2. Apparatus Description

While the main components will be described in further detail, several of the smaller components of the CAVIC require little description. These elements include pumps, hoses and connectors, adjustment valves and gauges and filter housings. Two of the smaller components will be described because of the important functions they perform relative to the principal requirement of non-intrusive testing. These components are the inhaler enclosure and the makeup airflow entrainment tube.

3.2.1. MOUDI Impactor

The cascade impactor incorporated in the CAVIC is a Multi-Orifice Uniform Deposit Impactor (MOUDI) produced by MSP Corporation (Minneapolis, MN). The MOUDI impactor has several features that make it more desirable to use than the Anderson impactor recommended by the USP. It has additional impactor stages for a more accurate MMAD calculation, as well as sharper impactor cut-offs (i.e. more ideal efficiency curves) for greater particle classification accuracy. It also has smaller impactor plates that use disposable aluminum foil covers for easier impactor cleaning and chemical work-up. The MOUDI impactor operates at 30 liters/minute. While the MOUDI impactor is more convenient to use than the Anderson impactor, the CAVIC could also operate with the Anderson impactor with just a simple flow rate adjustment.

3.2.2. Virtual Impactor

A virtual impactor functions very similar to a conventional impactor stage except that the larger particles "impact" into a slower moving airflow as illustrated in Figure 3.1. The incoming airflow is accelerated through a nozzle directly into a slower moving "minor flow". The larger portion of the total flow must turn abruptly away from the minor flow and becomes the "major flow". As with a conventional impactor stage, the larger particles with Stk greater than about unity will "impact" into the minor flow while the particles with smaller Stk will be able to follow the air streamlines into the major flow. The main difference between a virtual and conventional impactor is that the particles larger than the virtual impactors cut-off are carried away by the minor flow rather than being impacted onto a collection plate. This offers the advantage of being able to further study the large particles that were separated from the major flow.

The CAVIC uses two virtual impactor stages with cut-sizes of 10μm and 1μm. These impactors are part of a customized Model 310c Universal Air Sampler produced by MSP Corporation (Minneapolis, MN). The minor flow of the 10μm virtual impactor (i.e. containing particles larger than 10μm) is filtered of drug particles and the major flow is directed to the 1μm virtual impactor. The major flow of the 1μm virtual impactor (i.e. containing particles smaller than 1μm) is filtered of particles and the minor flow is directed to the MOUDI impactor for further classification. This airflow setup is illustrated in Figure 3.2. Since it is expected that most inhalers will produce aerosols with MMADs in the range

of 1-5μm the collection of particles larger than 10μm and smaller than 1μm on filters should not adversely affect the accuracy of our measurement of MMAD.

The total flow rate of the CAVIC is 300 liters/minute. This enables the testing of inhalers at flow rates higher than were previously available, as well as with flow patterns with high flow rate peaks.

3.2.3. Mouth and Throat

A realistic molded fiberglass mouth and throat assembly is used instead of the USP induction port. This assembly closely resembles the actual extra-thoracic airways and is presented in Figure 3.3. The mouth and throat assembly is used for two reasons: it provides the change of flow direction also accomplished by the USP induction port and it more closely mimics the actual particle deposition that would occur during *in vivo* use. This enables the aerosol measurements taken by the cascade and virtual impactors to resemble more closely the aerosol delivered to the lungs. The mouth and throat assembly separates into two halves to accommodate easier cleaning, surface coating and chemical work-up.

3.2.4. Happy Breathing Machine

All the inhalation flows used with the CAVIC are produced by a precisely controlled piston. The piston is driven by a stepper motor, which is in turn controlled by a personal computer. This breathing apparatus is called the Happy Breathing Machine (HBM) and is capable of producing inhalation or exhalation flows as well as constant or variable flow rates and single or cyclic breaths. Cyclic flows can have different inhalation and exhalation profiles provided they have the same volume. Flow rates from 0.1 to 280 liters/minute are possible. The HBM was designed by Brit Hennig, with significant improvements by Cam Shute, both previous summer students.

3.2.5. Inhaler Enclosure

To enable the inhaler to be sampled with realistic breath patterns, without excessive loss of drug particles, it was necessary to force air through the back of the inhaler with a positive pressure, rather than draw air through the mouthpiece of the inhaler with a vacuum pressure. This was easily accomplished by setting the HBM to "exhale" the breathing pattern rather than "inhale".

The differential pressure across the device, which causes the movement of air and the atomization process, remains constant whether drawing through the mouthpiece or

forcing air through the back of the device. Since the drug consists of a dry powder and the flow is low speed, the absolute pressure of the air will not effect the process. The inhaler enclosure seals around the mouthpiece of the inhaler to ensure that the exhaled breathing pattern applied to the back of the device will flow in a manner identical to an inhaled breathing pattern applied to the mouthpiece. The inhaler enclosure is diagrammed in Figure 3.4.

3.2.6. Makeup Airflow Entrainment Tube

All impactors require a constant flow rate through them to function. This is required to maintain calibrated cut-sizes for the impactor stages. This is the main reason the USP procedure tests inhalers at a constant flow rate. To facilitate testing of inhalers with varied flow patterns it was necessary to have an impactor with a flow rate that exceeded the flow pattern's maximum flow. The generated aerosol could then be blown into this high, constant flow rate at arbitrary rates as long as makeup air was readily provided.

With a goal of non-intrusive aerosol collection, it is important to minimize the turbulence, and therefore the possibility of deaggregation, during the entrainment of the aerosol flow. To do this without producing unnecessary turbulence, the velocities of the two flows must match. This is impossible for varying flow rates and fixed diameter flow tubes, so the diameter of the flowtubes was chosen to match average velocities. This maintains a minimum flow rate difference between the makeup and entraining aerosol flow over a wide range of entraining flow rates.

The two airflows are also brought together at a shallow angle, again to try to minimize production of turbulence. The makeup airflow entrainment tube is also illustrated in Figure 3.4.

3.3. Setup and Procedures

Other than adjustments required to accommodate the differences in equipment and inhalation profiles, the procedure used is meant to follow the USP guidelines as closely as possible, and is as follows.

Ensure the mouth and throat assembly and the impactor plates are clean and free of residual silicon coating left over from the previous run. Install disposable aluminum foil discs onto the impaction plates and secure the retention rings. Apply a thin layer of spray-on liquid silicon coating to the interior surfaces of the mouth and throat assembly and to each impactor plate. The silicon should be applied in two coats, with sufficient time between coats

for the propellant to completely evaporate. When the propellant of the second coat has completely evaporated, assemble the two halves of the mouth and throat and the MOUDI impactor stages, making sure all edges and stages are properly sealed. Install collection filters into and assemble the 10μm and 1μm virtual impactors. Connect the MOUDI impactors inlet and outlet to the appropriate virtual impactor hoses. Install the inhaler into the front half of the inhaler enclosure and attach to the mouth and throat assembly. Install the mouth and throat assembly into the makeup airflow entrainment tube as illustrated in Figure 3.4, making sure all joints are sealed. Connect the back half of the inhaler enclosure to the HBM hose and load the appropriate breath pattern. Turn on the CAVIC vacuum pumps and check gauges to ensure proper flow rate calibration. Adjust flow rates if needed. Load the drug dose into the inhaler, assemble the inhaler enclosure and run the HBM breath pattern. If additional doses are required for the sample, separate the inhaler enclosure halves, reset the HBM breath pattern and load the inhaler for the next dose. Allow the vacuum pumps to run for an additional 20 seconds after the last dose has been actuated to allow for complete drug collection. Turn off the pumps and the HBM and dis-assemble all the parts. Wash with solvent and dilute to an appropriate volume the inhaler mouthpiece, mouth and throat, all the impactor stages and end filter and the two virtual impactor filters. Determine the mass of drug collected in each component by using the specified method from the drug monograph. Determination of drug mass is done with a UV spectrophotometer.

3.4. Size Determination

Calculation of MMAD and GSD follows the procedure outlined in the USP with a few modifications to accommodate the use of two virtual impactor filters. The modifications in calculating procedure deal solely with allocating the additional sources of collected drug onto the appropriate impactor plate.

The most trivial solution would be to add the amount of drug collected on the 10μm virtual impactor filter to the amount of drug collected on the 9.9μm MOUDI impactor plate and the drug collected on the 1μm virtual impactor filter to the impactor stage below the 1μm MOUDI impactor plate. This is not an acceptable solution because of the collection efficiencies of virtual impactors. Virtual impactors, in general, have collection efficiency curves that are far from ideal, having a relatively shallow slope rather than the ideally steep-sloped curve. For this reason, the drug collected on the virtual impactor filters is allocated to more than one MOUDI impactor plate.

Ideally, the drug collected on the filters could be allocated to each impactor plate based entirely on the collection efficiency curve for the corresponding virtual impactor. However, this would require knowledge of the particle size distribution entering each virtual impactor. Since this is unknown, we use the best approximation available, the distribution measured with the MOUDI impactor. Therefore, the solution to allocating the filter contents uses the relative amounts of drug collected on the MOUDI impactor plates, modified by the efficiency curve data, to determine drug allotment amounts for each affected impactor plate. This amount is calculated using

$$mx_n = \frac{m_n}{CE_n} * \frac{mf}{\sum_{n=l}^{s} \frac{m_n}{CE_n}} \qquad (3.1.)$$

where

m = drug mass
mx = additional drug mass for allocation to the impactor plates
mf = total drug mass on virtual impactor filter
CE = collection efficiency of the virtual impactor at the impactor stage cut-size

and subscripts

n = impactor stage
l = largest impactor stage to have drug allocated from filter mf
s = smallest impactor stage to have drug allocated from filter mf.

Equation (3.1) is applicable for each impactor stage that will have additional drug allotted to it.

The only MOUDI plates that will receive additional drug from the 10μm virtual impactor filter are the 9.9μm and 18μm plates. Since greater resolution of impactor data for particles over 10μm provides no additional information in the calculations of MMAD or GSD, all the drug collected from the 10μm virtual impactor filter and the drug collected on the 18μm MOUDI plate were added to the amount of drug collected on the 9.9μm MOUDI plate. This helped to simplify the calculations somewhat.

Four stages of the MOUDI impactor will receive additional drug from the 1μm virtual impactor filter. These are the 1.8μm, 1.0μm, 0.524μm impactor plates and the final filter. The ratios of drug allotted to each of these stages is dependent upon the size distribution of the MOUDI collected drug and will vary slightly from test to test.

Once the modified drug amounts for each MOUDI impactor stage are determined, the MMAD and GSD are calculated using the same method as outlined in the USP.

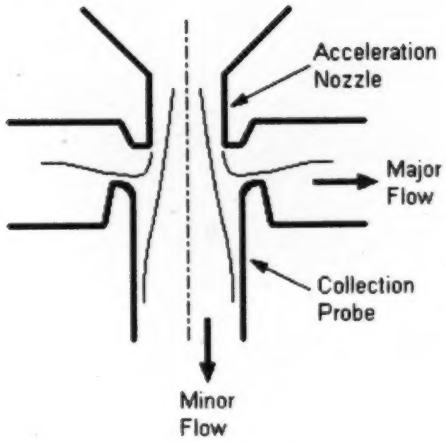

Figure 3.1. Virtual Impactor stage

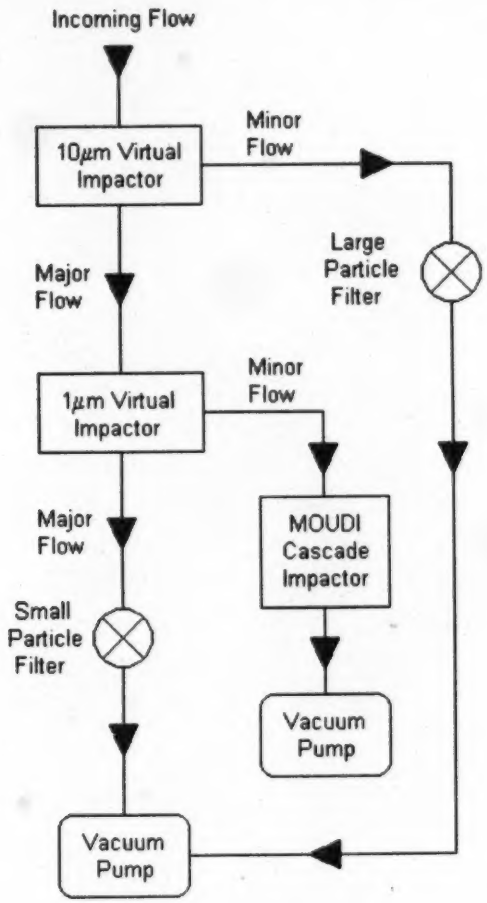

Figure 3.2. Flow diagram of the CAVIC

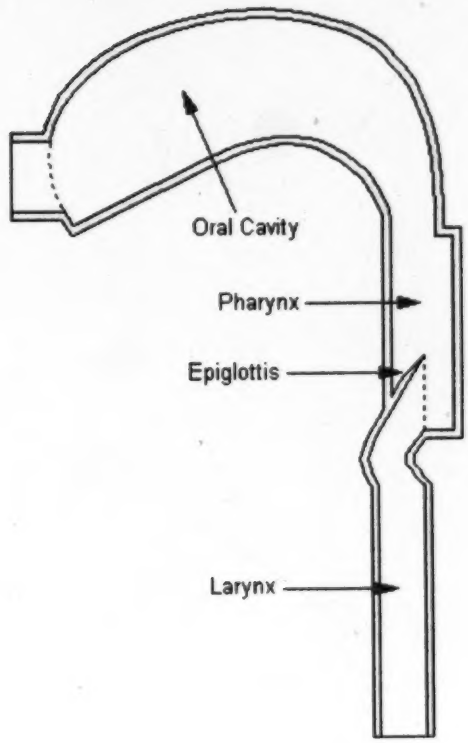

Figure 3.3. Realistic mouth and throat assembly

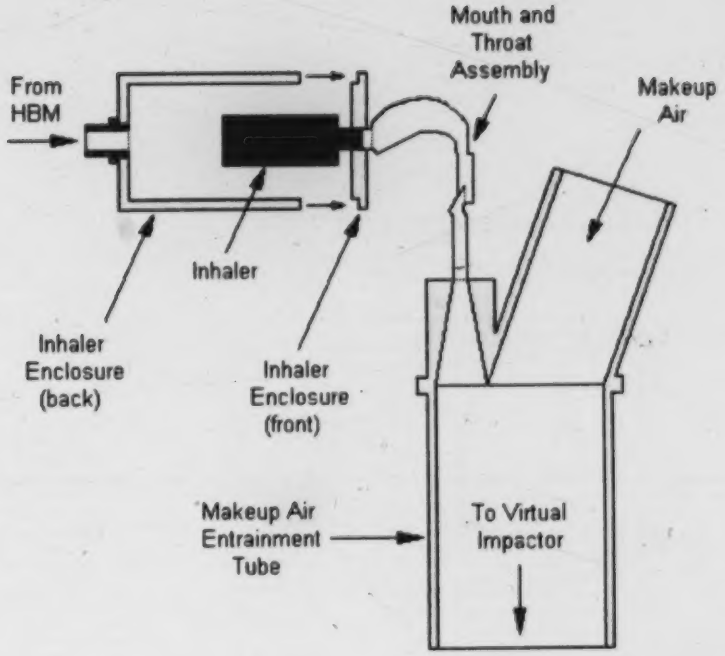

Figure 3.4. Upper CAVIC assembly diagram

4. Validation

4.1. Introduction

The purpose of validation is to scrutinize the CAVIC to ensure it performs as expected. The principle expectation of the CAVIC introduced in the previous section is the preservation of the aerosol particle size. As discussed earlier in section one, a dry powder aerosol is produced by dispersion of a finely milled drug powder into individual or small agglomerates of particles. The size of the individual particles and the amount of particle separation accomplished by the inhaler are what determine the size distribution of the aerosol. To validate the CAVIC it is essential to show that the aerosol collection and classification process does not further separate the agglomerated drug particles in the aerosol being collected, and thus alter the size distribution of the aerosol. This feature can be validated by theoretical analysis of the CAVIC design and by experimental comparison of the CAVIC to a currently accepted measuring device. The purpose of this chapter is to describe the work we have done to validate the performance of the introduced CAVIC.

4.2. Analytical Validation

The forces that act upon airborne particles have been reviewed in the literature (e.g. Israelachvili (1992)). French *et al.* (1996) apply these concepts specifically to dry powder inhaler aerosols. For dry, uncharged, nonhygroscopic particles, the force holding the particles together is the Van der Waal's interparticle force, f_v, which for spherical particles of like diameter is given by

$$f_v = \frac{A \cdot d}{6 \cdot h^2} \tag{4.1}$$

where A is the Hamaker constant and h is the distance separating the two attracted particles. The value of A is dependent upon the molecular composition of the particle surface and ranges between 10^{-19} and 10^{-20} J.

In addition to the Van der Waal's forces, the gravitational body force, f_g, acting on a spherical particle is given by

$$f_g = \frac{\pi \cdot p_{part} \cdot g \cdot d^3}{6} \tag{4.2}$$

where p_{part} is the density of the particle and g is the gravitational constant.

French *et al.* (1996) also summarized that separation of agglomerated drug particles is brought about by viscous stresses produced by eddies within a turbulent flow. These stresses are brought about by the large velocity gradients that exist in small turbulent eddies present in turbulent flow. This viscous force, f_{vis}, can be estimated by

$$f_{vis} = 4 \cdot \pi \cdot d^2 \cdot \mu \cdot \frac{v_{turb}}{l_{turb}} \tag{4.3}$$

where

d = drug particle diameter;
μ = dynamic viscosity of the gas;
v_{turb} = characteristic velocity scale;
l_{turb} = characteristic length scale.

One force that can also cause separation of agglomerated drug particles, which French *et al.* (1996) neglected, is the acceleration force exerted on a particle as it moves between different turbulent eddies. This force, f_{acc}, can be estimated by

$$f_{acc} = \pi \cdot p_{part} \cdot d^3 \cdot \frac{(v_{turb})^2}{(6 \cdot l_{turb})} \tag{4.4}$$

Using the values presented in Table 4.1 (values for A and h are as recommended by French *et al.* (1996)), equations (4.1) and (4.2) give $f_v = 6.7 \times 10^{-5}$ d and $f_g = 5137\ d^3$ in S.I. units. Therefore, Van der Waal's forces will dominate, $f_v \gg f_g$, when $d \ll 100\mu m$ and gravitational forces will dominate, $f_g \gg f_v$, when $d \gg 100\mu m$. This allows us to simplify our comparison by neglecting the gravitational force and considering only Van der Waal's and fluid forces. In this case, for deaggregation of agglomerated drug particles to occur we require

$$f_{vis} \gg f_v \tag{4.5}$$

or

$$f_{acc} \gg f_v. \tag{4.6}$$

For easier comparison these can be stated as separatory force ratios: $f_{vis}/f_v \gg 1$ or $f_{acc}/f_v \gg 1$.

Before f_{vis} and f_{acc} can be calculated it is necessary to estimate the length and velocity scales of the turbulent eddies. Scales from the largest eddies in a fluid flow are called integral scales, while those from the smallest eddies are called Kolmogorov scales. Integral length and velocity scales in a turbulent jet can be estimated (e.g. Tennekes & Lumley (1972) or White (1974)), respectively, by

$$l = 3 \cdot D \tag{4.7}$$

and

$$u = 0.074 \cdot u_{noz} \cdot \sqrt{\pi \cdot 0.06} \tag{4.8}$$

where D is the jet diameter and u_{noz} is the flow velocity through the jet nozzle. Kolmogorov length and velocity scales in a turbulent jet can be estimated, respectively, by

$$\eta = \left(\frac{l \cdot \nu^3}{u^3} \right)^{1/4} \tag{4.8}$$

and

$$v_{kol} = \left(\frac{\nu \cdot u^3}{l} \right)^{1/4} \tag{4.10}$$

where ν is the kinematic viscosity of the fluid.

Since these scale estimates depend on the geometry of and flow rate through the nozzle, distinct calculations were done for every impaction stage of the CAVIC. Using the values presented in Table 4.1, the separatory force ratios for each impaction stage were calculated and are presented in Table 4.2. Since each impactor stage is exposed to a range of particle sizes, a typical diameter was used. While French *et al.* (1996) used a combination of scales that represented the 'worst case scenario' in their force calculations, they mistakenly used length and velocity scale estimates from different sized eddies. We calculated the separatory forces using both eddy size scales but only the results from the Kolmogorov scales are given as they present the more critical comparison. As presented in Table 4.2, only the 1μm virtual impactor presents any reasonable possibility of causing further deaggregation of the drug aerosol particles.

Combining equations (4.1) and (4.4) into equation (4.6) and solving for particle diameter gives

$$d \gg \sqrt{\frac{A \cdot l_{turb}}{\pi \cdot p_{part} \cdot h^2 \cdot v_{turb}}} \tag{4.11}$$

A = Hamaker Constant	1.00×10^{-20} J
g = gravitational constant	9.81 m/s^2
h = interparticle distance	5.00×10^{-9} m
μ = dynamic viscosity	1.80×10^{-5} kg/m.s
ρ_{part} = particle density	1000 kg/m^3
ν = kinematic viscosity	1.50×10^{-5} m^2/s

Table 4.1. Values of Parameters.

Stage	Typical Diameter (μm)	f_{vis} / f_v	f_{acc} / f_v
0	18	0.0013	0.0010
1	14	0.0019	0.0015
2	8.4	0.0028	0.0021
3	6.6	0.0029	0.0019
4	5.3	0.0052	0.0042
5	3.8	0.0074	0.0060
6	2.5	0.0135	0.0119
7	1.4	0.0259	0.0239
8	0.76	0.0389	0.0326
VI 10μm	18	0.0271	0.0920
VI 1μm	5.5	0.5904	5.1785

Table 4.2. Ratios of particle forces for each MOUDI impactor stage and virtual impactor stage.

which is useful for determining what sizes of particles are susceptible to deaggregation for each impactor stage. Using the values in Table 4.1 and substituting equations (4.9) and (4.10) for the Kolmogorov scales into equation (4.11) gives the particle diameters presented in Table 4.3. Comparing the impactor stage cutoff diameters with the calculated critical diameters in Table 4.3 also indicates that the 1μm virtual impactor stage is the only one where further deaggregation could occur. This comparison also indicates that only the larger particles in the size range that enter the 1μm virtual impactor could be acted on by forces sufficient to cause deaggregation. Aerosols with MMADs larger than the critical 2.4μm size would be affected more than aerosols with smaller mass median diameters.

Unfortunately, these theoretical validation calculations do not indicate the extent of deaggregation that can occur, or predict the effect, if any, on the aerosol's size distribution. This requires that experimental validation be used to determine whether the deaggregation effects are significant.

Stage	Particle Diameter Range (μm)	Critical Particle Diameter (μm)
0	> 18	583
1	9.9 – 18	360
2	6.9 – 9.9	182
3	6.2 – 6.9	150
4	4.4 – 6.2	82
5	3.1 – 4.4	48
6	1.8 – 3.1	23
7	1.0 – 1.8	9.0
8	0.524 – 1.0	4.2
VI 10μm	> 10	59
VI 1μm	1 – 10	2.4

Table 4.3. Critical diameter of an agglomerated drug particle for deaggregation to occur as a result of acceleration forces in turbulent eddies. Particle clumps larger than the critical diameter are susceptible to deaggregation.

4.3. Experimental Validation

While analytical investigation offers an approximate indication of possible particle deaggregation, it does not provide any information on the effect this could have on measured MMAD. This requires that aerosol measurement data be included in the apparatus validation process. The measuring device under study can be shown not to cause particle deaggregation if it presents equivalent aerosol size distribution data compared to a device known to be accurate.

Our experimental validation compared distributions measured with the CAVIC to an uncoupled MOUDI impactor. Three different dry powder inhalers were used in the comparison to address a range of aerosol distribution sizes. The inhalers used were the Spiros (Dura Pharmaceuticals, San Diego, CA, USA), the Turbuhaler (Astra Pharmaceuticals Inc., Mississauga, ON, Canada) and the Ventodisk (Glaxo Canada Inc., Toronto, ON, Canada). The Spiros and Ventodisk were both loaded with salbutamol sulfate powder formulation while the Turbuhaler was filled with terbutaline sulphate powder. While different drugs were used to try and address a variety of particle size ranges, all the inhalers tested incorporated lactose in the formulation to act as a drug carrier. Each device went through the same series of experiments, which consisted of five "runs" on each measurement setup (i.e. five runs using the MOUDI and five runs using the CAVIC). Each run consisted of collecting a

number of doses of drug from the inhaler device. Each dose was "inhaled" by the collection device at a constant flow rate of 30 liters/min. This flow rate was established by the calibration requirements of the MOUDI.

The number of doses collected for each run varied from one device to the next, but was chosen as the minimum number of doses that still produced sufficient chemical concentrations for reliable assay results. Typically three doses were collected for each run and this provided an average MMAD for the run. Minimal doses were used with each run to avoid overloading the impactor. Overloading occurs when the sampled aerosol introduces a larger number of particles in a certain size range than the collection device is able to completely collect. With dry powders, this typically occurs when the silicon or other collection substrate becomes saturated by the aerosol powder and further introduced particles of equal size bounce off the loaded substrate and collect on the following impactor stage. An additional five runs on the MOUDI impactor were collected with high doses to ensure overloading was not occurring. Overloading would be evidenced by a shift in the MMAD of the overloaded samples when compared to non-overloaded samples. This shift in measured size distribution would also be evidenced between two runs of different dose that were both overloaded.

The results of the validation are presented graphically in Figures 4.1 to 4.4. Each figure presents the averaged cumulative size distributions of the sets of runs being compared. The vertical bars represent the standard deviation of each impactor stages 5-run averaged data. The results were also compared statistically, to emphasize any significant differences that might exist between the distributions being evaluated. Analysis of variance (ANOVA) was employed to enable comparisons of more than two data sets simultaneously. The statistical analysis consisted of testing the MMADs and GSDs of the five runs for each test set. As discussed earlier, size distributions of aerosols are often log-normally distributed, so the logarithms of the MMAD and GSD were used in the analysis. This transformation was done to have values more closely resembling a normal distribution in the statistical analysis.

4.3.1. Ventodisk

As the Ventodisk was the first device to be used in the validation, the CAVIC to MOUDI and loading comparisons were done as two independent comparisons. Experimental parameters such as drug lot and environmental conditions differed between these two comparisons so no attempt was made to relate one comparison to the other.

Figure 4.1 presents the results of the CAVIC and MOUDI comparison. Three doses of drug were used for each experimental run. As can be seen in Figure 4.1, both sets of data are very similar. Statistical analysis showed that there is no significant difference between the MMAD of the distributions obtained by each measurement device (ANOVA, $P>0.01$). Additionally, no significant difference could be shown statistically between the GSDs of the distributions (ANOVA, $P>0.01$). These results indicate that the CAVIC does not cause further deaggregation of the drug particles produced by the Ventodisk inhaler.

Figure 4.2 presents the results of the loading validation using the Ventodisk inhaler. The two sets of data used two and three doses of drug respectively per run. Figure 4.2 shows that both sets of data are very similar. Statistical analysis also showed that there is no significant difference between the MMADs or the GSDs (ANOVA, $P>0.01$). This affirms the validity of the CAVIC and MOUDI comparison by demonstrating that no overloading had occurred.

4.3.2. Spiros

The validation using the Spiros device incorporated the CAVIC to MOUDI and loading comparisons all in one experiment. The CAVIC and regular MOUDI runs used three doses of drug while the loading runs used five doses. Figure 4.3 presents graphically the averaged cumulative size distribution of all the experimental runs for the Spiros inhaler. As can be seen in Figure 4.3, all three sets of data are very similar to one other. Additionally, statistical comparison showed that there is no significant difference between the MMADs or GSDs of each distribution (ANOVA, $P>0.01$). These results indicate that no overloading occurred during the experiment and that the CAVIC does not cause further deaggregation of the drug particles produced by the Spiros inhaler.

4.3.3. Turbuhaler

Validation using the Turbuhaler device also incorporated both comparisons in one experiment. The CAVIC and regular MOUDI runs used five drug doses and the loading MOUDI runs used 10 doses. Figure 4.4 presents the averaged distributions of all the experimental runs for the Turbuhaler. As can be seen in Figure 4.4, all three sets of data seem substantially different. Statistical comparisons confirm that there is a significant difference between the MMADs and GSDs of the distributions (ANOVA, $P<0.01$). Specifically, the MMAD and GSD measured using the CAVIC differs significantly from the regular runs measured using the MOUDI (Student's t-Test, $P<0.01$). In spite of the apparent

large difference between the regular and loading runs on the MOUDI, statistically there is no significant difference between the MMAD and GSD (Student's *t*-Test, $P>0.01$) of these runs. This is a result of the very large variance between the several runs. These results indicate that no significant overloading occurred during the experiment but that the CAVIC does not adequately measure the size distribution of the aerosol produced by the Turbuhaler inhaler.

The CAVIC fails in this instance because of the excessive number of large drug particles produced by the Turbuhaler. As can be seen in Figure 4.4, between 39% and 65% of the aerosol mass that was collected is in particles over 10μm in diameter. Some of these particles were estimated to be as large as 500 μm. Aerosol particles this large tend to impact on the inside of the CAVIC device because of the dominance of gravitational forces. While some of these deposited drug particles could still be collected from the accessible surfaces by washing, other deposition surfaces were inaccessible. The drug deposited on these surfaces was counted as "losses", and caused the typical drug losses to exceed acceptable levels. Significant loss of very large drug particles in the MOUDI impactor did not occur.

The aerosol size distributions in Table 4.3 also indicates that significant particle deaggregation could occur within the CAVIC. This finding is supported by the analytical validation as the aerosol generated by the Turbuhaler had a MMAD that greatly exceeds the 1μm virtual impactor critical particle diameter. This finding is not refuted by the results from the Ventodisk and Spiros inhalers as these devices has sufficiently small MMADs that any deaggregation that could have occurred would be insignificant. However, since the CAVIC was unable to sufficiently collect the Turbuhaler aerosol samples, it cannot be stated without reservation that the difference in measured MMAD was caused solely by deaggregation. Further validation, which was not undertaken as part of this experiment, would have to be completed to determine if deaggregation was significant for certain particle sizes in the 1μm virtual impactor stage.

This portion of the validation process exposed one deficiency of the CAVIC i.e. its inability to adequately collect very large particles. This deficiency makes it impossible to validate the CAVIC against deaggregation of all particle sizes. It is, therefore, necessary to validate each device to be used with the CAVIC before testing can continue. The CAVIC was shown to have no significant deaggregation with the Ventodisk and the Spiros devices, so they were both used in the principle tests with realistic inhalation profiles. Since it was not shown that the CAVIC could measure the Turbuhaler's aerosol reliably, the Turbuhaler was not used in the principle tests outlined in this document.

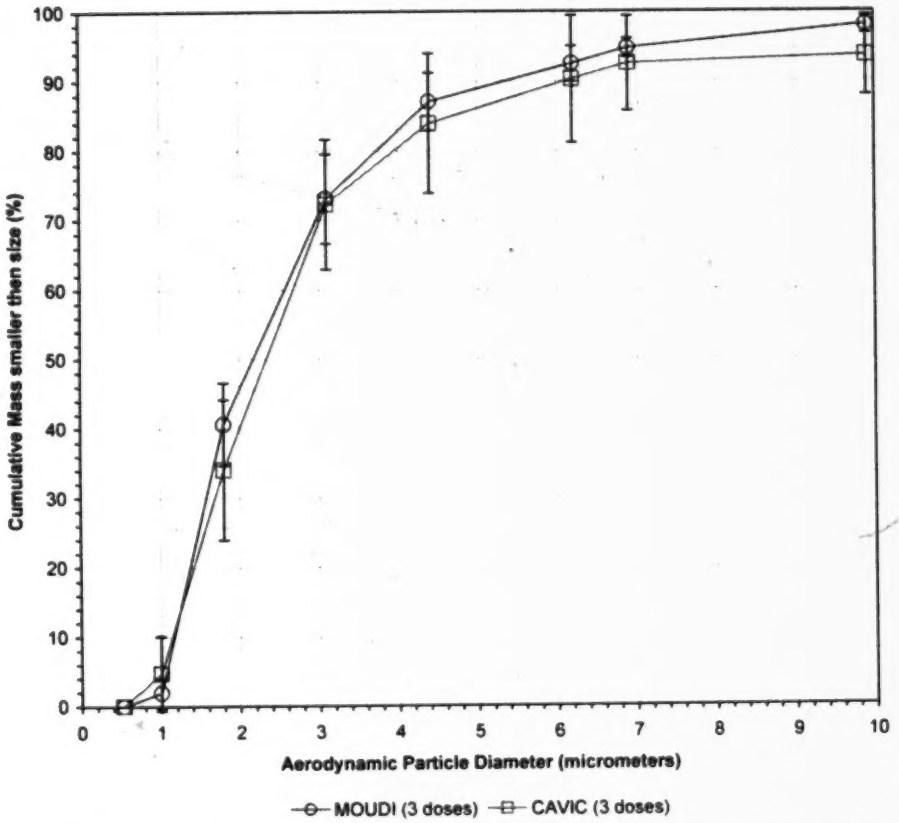

Figure 4.1. Size distributions measured by the MOUDI and CAVIC impactors for validation of the Ventodisk inhaler.

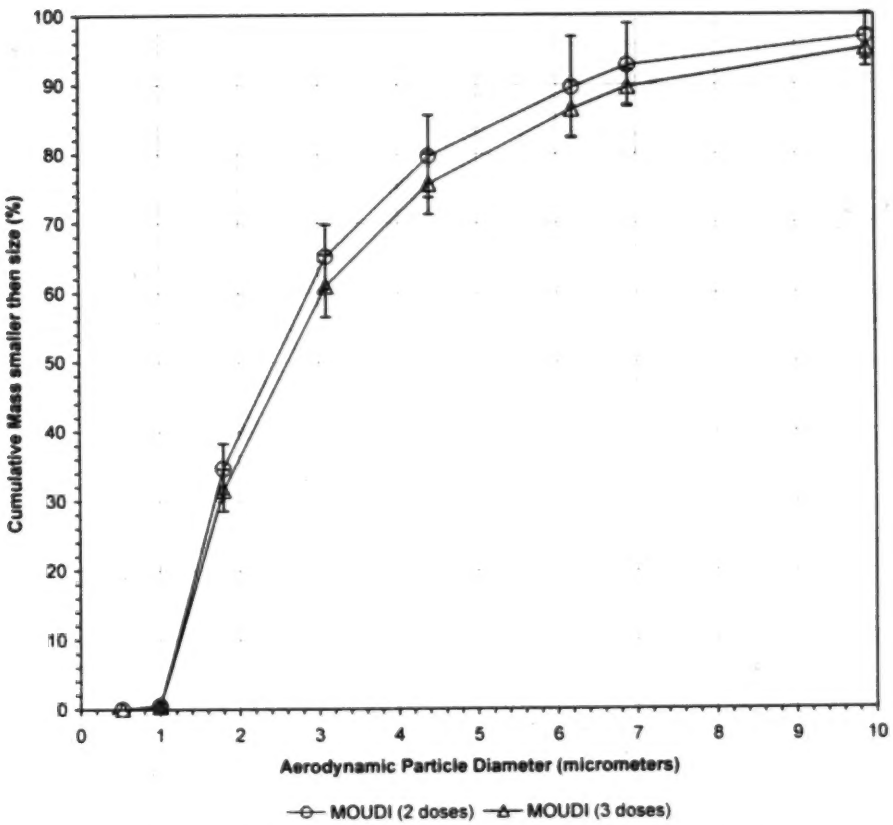

Figure 4.2. Size distributions to check for overloading for validation of the Ventodisk inhaler.

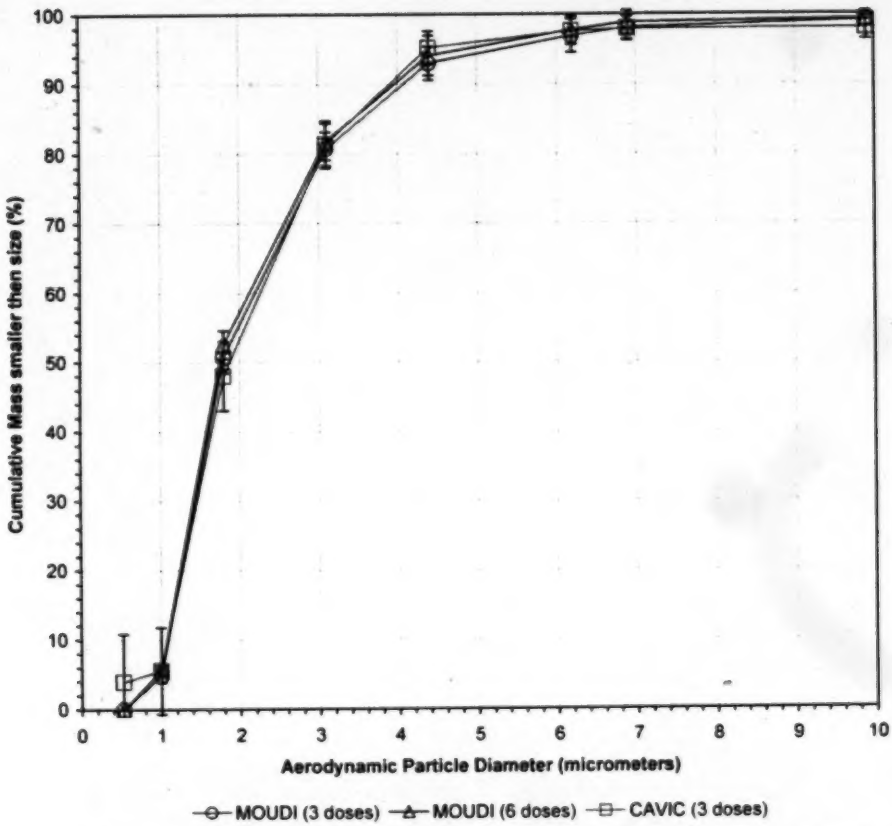

Figure 4.3. Size distributions measured by the MOUDI and CAVIC impactors for validation of the Spiros inhaler.

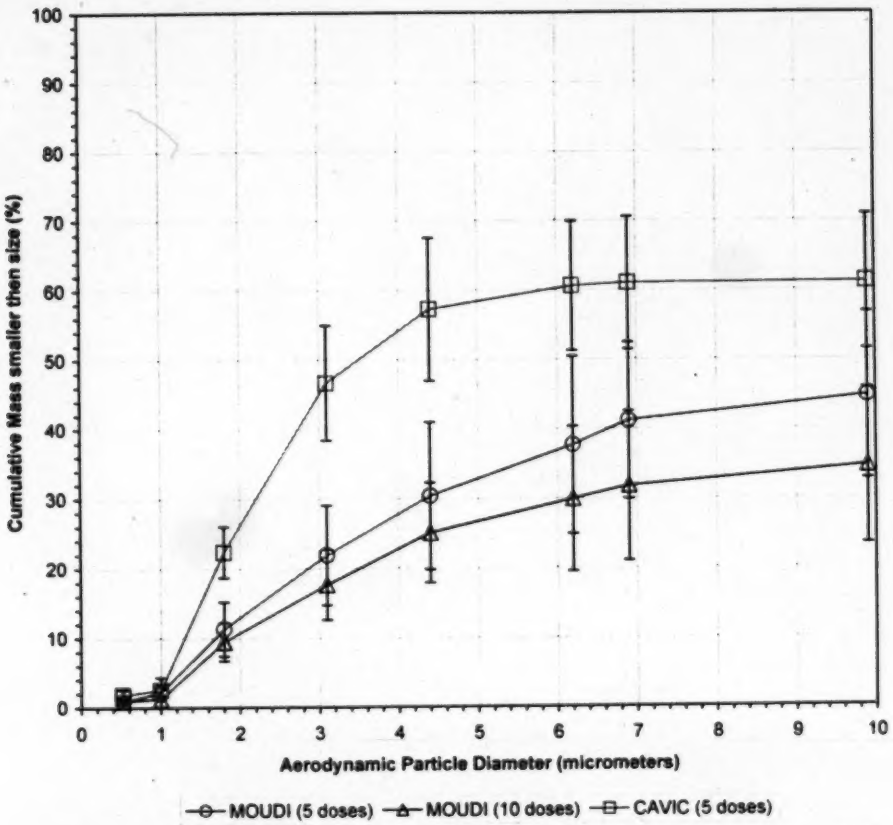

Figure 4.4. Size distributions measured by the MOUDI and CAVIC impactors for validation of the Turbuhaler inhaler.

5. Plethysmograph and Breathing Data

5.1. Introduction

In order to successfully compare current inhaler testing methods to techniques that more closely resemble actual use of the inhaler, it is essential that the air flow through the inhaler simulates the inhalation pattern of an actual user while operating that device. This chapter will describe the apparatus used to measure real inhalation patterns and present the patterns used in the comparison test described later in this work.

5.2. Plethysmograph

A plethysmograph is a device that transduces changes of volume into air pressure changes. This is done by enclosing the test subject in a sealed container and measuring the pressure change inside the enclosure as the subject's volume changes. These air pressure changes can than be recorded as changes over time. By measuring the changes in volume of a person's body as they inhale and exhale, a breathing profile can be determined.

5.2.1. Apparatus Description

The plethysmograph used in this study seals an individual inside an air tight box with their head protruding, as demonstrated in Figure 5.1. One side of the box is removable to enable entry and exit. A neoprene neck piece seals around the individuals neck and prevents air leakage. Air pressure changes produced by the individuals breathing are measured with a pressure transducer, fastened to the rear of the box, and an oscilloscope, which records the transducer output at a specified frequency and saves this data to floppy disc. The oscilloscope display screen provides a real time presentation of the measured data, which is usually of great interest to the test subject. The plethysmograph also has an external syringe cylinder attached that is used for volume calibration. As the residual volume of air

inside the box differs for each test subject, it is required to provide calibration data for each subject tested. The plethysmograph was based on a design kindly supplied by Professor D. Jones (Dept. of Medicine).

5.2.2. Operational Procedure

It was required that the test subjects push their head through the neck piece as they entered the plethysmograph. Spacers were provided for the subject to sit on to adjust for differences in torso height. The side of the box was then replaced and sealed and the neck piece was checked to ensure it also sealed properly. Using the syringe cylinder, a fixed volume (1 liter) of air was injected into the sealed enclosure while the test subject held their breath to avoid additional volume changes. The difference in pressure transducer output was recorded during this air injection and was used for calibration of the conversion between transducer output voltage and inhaled volume. The test subject was then read the manufacturers instructions for proper use of the test inhaler device and was allowed several test breaths through the device to become comfortable with its use. Inhalation patterns were then recorded and saved while the subject operated the inhaler device, simulating its use. The same procedure was then followed using a second inhaler device, so that inhalation patterns through two different devices was obtained for each subject tested. The devices used were the Ventodisk and the Spiros dry powder inhalers also used in the validation section of this work. These devices had no drug cartridges installed during this procedure and had been washed to ensure no drug residue remained in the device.

The pressure data displayed by the oscilloscope is the voltage output of the pressure transducer. No attempts were made to zero the voltage reading as any zero point would be arbitrary. These readings were sampled at 100 Hz to ensure the data would be smooth and accurately detail the flow rate fluctuations. This voltage data was then formatted, smoothed to eliminate resident noise and then transformed into volume using the calibration data obtained from each volunteer. This was accomplished using pre-existing software programs designed specifically for this purpose. ("cnvrtwfm.exe" and "single.exe", Cam Shute, July, 1997) This volume data could then be plotted and viewed to assist in breath pattern comparisons. Example breath plots are shown in Figures 5.2 to 5.3. The transforming software also produced instantaneous flow rate data for each data point. Once the desired breath pattern was identified, a different software program was used to transform the corresponding flow rate data into inhale and exhale data files for use with the Happy Breathing Machine ("mkcurv.exe", Cam Shute, July, 1997).

Volunteer	Gender	Age
1	Male	6
2	Female	8
3	Male	9
4	Male	10
5	Female	12
6	Male	13
7	Female	14
8	Male	14
9	Female	15
10	Male	17

Table 5.1. Distribution of age and gender among the volunteers involved in the breath pattern survey.

5.3. Breath Patterns

The breathing patterns used in this work were obtained from volunteer subjects. All the volunteers involved in the breathing pattern survey experienced chronic pulmonary disorders or asthma and they all had previous experience using inhaler devices. The ten volunteers surveyed ranged from 6 to 17 years in age and were comprised of 4 females and 6 males as outlined in Table 5.1. Each subject provided at least two recorded breaths for each device: the Ventodisk and the Spiros for over 40 patterns collected. Various ages and genders were utilized in the breath survey to provide a wide variety and set up an approximate range of inhalation patterns. From this range, maximum and minimum breaths were chosen. This enabled us to approximate the upper and lower limit of breathing pattern that would be used at the time of actual inhaler use.

The maximum and minimum breath patterns are referred to as the "fast" and "slow" patterns respectively. These patterns were chosen based on: peak flow rate, inhaled volume and acceleration of the flow rate at inhalation onset. Figure 5.2 shows the breathing patterns chosen for use with the Ventodisk device, while Figure 5.3 shows the breathing patterns chosen for use with the Spiros device. The zero volume point on both of these figures was arbitrarily chosen as the initial inhale volume. As can be seen in these two figures, the profiles of the Ventodisk breaths differ markedly from the Spiros breaths. This was expected based on the operational instructions of the two devices. While the Ventodisk instructions required a quick, deep breath through the device, the Spiros instructions called for a prolonged, slow, steady breath.

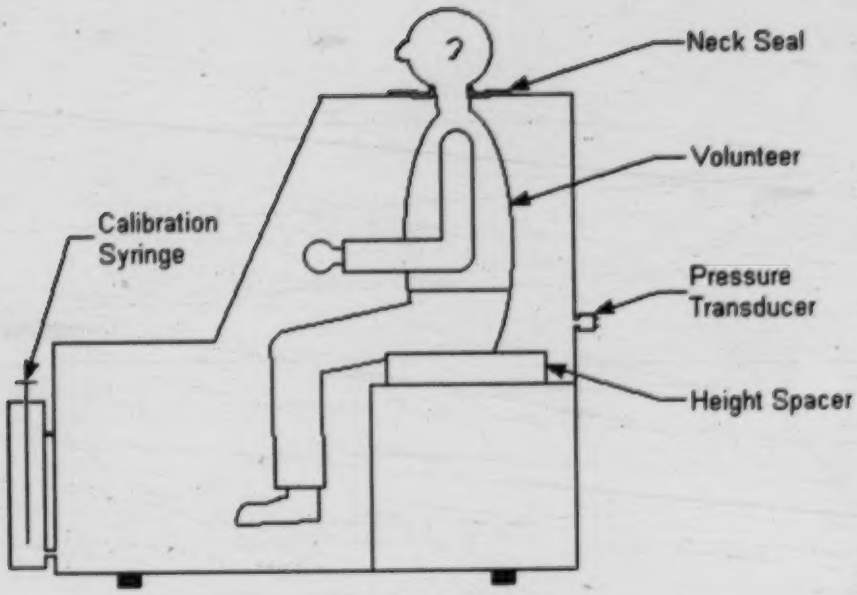

Figure 5.1. Schematic of the Plethysmograph

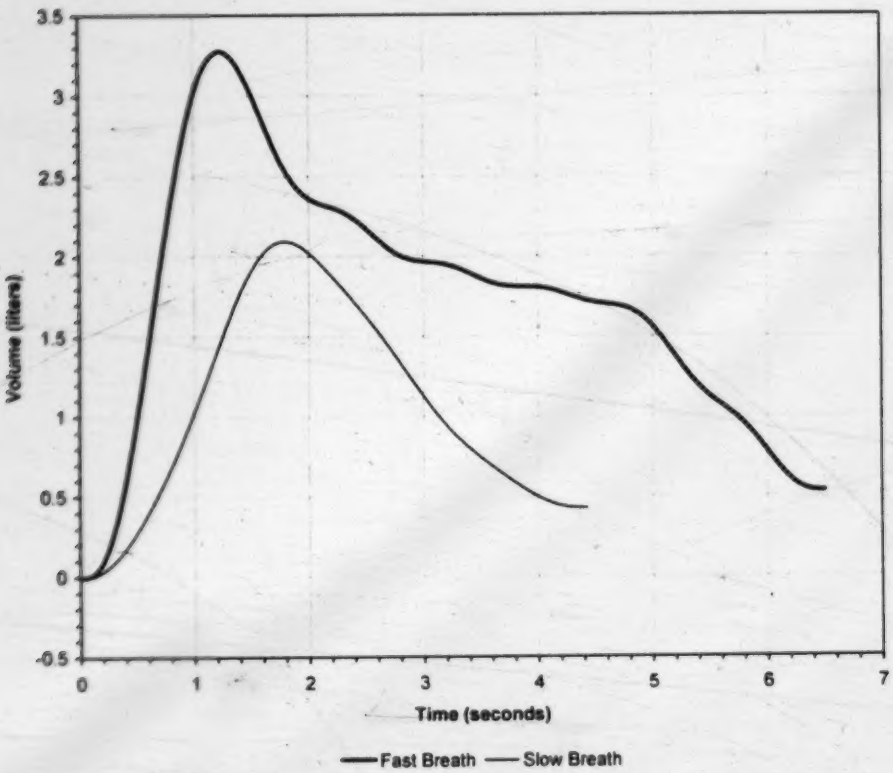

Figure 5.2. Breathing patterns that were generated and used with the Ventodisk dry powder inhaler.

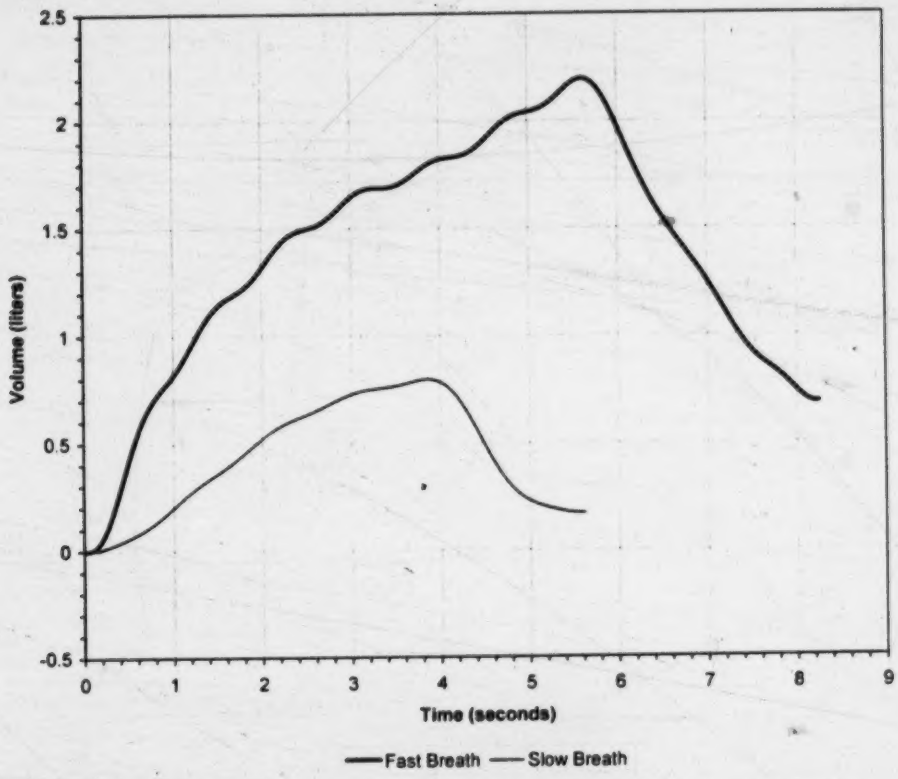

Table 5.3. Breathing patterns that were generated and used with the Spiros dry powder inhaler.

6. Tests and Results

6.1. Introduction

The main goal of the experiment described in this document is to compare the aerosol size distribution of dry powder inhalers when sampled using a realistic flow pattern to that obtained when using a constant flow rate. As discussed earlier, the inhalers being used are the Ventodisk and the Spiros. The purpose of this comparison is to determine if the currently accepted inhaler testing methods accurately predict the performance of these devices when used by an actual patient. This section will describe the comparative tests performed and present the results of the tests.

6.2. Flow Pattern Comparative Tests

The ideal experimental comparison would alter only the variable under study while keeping all other variables constant. To avoid altering the flow any more than necessary, the constant flows were matched to the breathing pattern flows as closely as possible. For the Spiros, each flow pattern was compared to its average flow rate, and for the Ventodisk, each pattern was compared to its average flow rate and one additional flow rate. The Ventodisk's slow breathing pattern was also compared to it's maximum flow rate, while the fast pattern was compared to 100 liters/min flow rate, which is a commonly used test flow rate, hereafter referred to as the USP (United States Pharmacopeia) flow. The maximum flow rate of the fast breathing pattern was not included in the tests because it exceeded the maximum flow capabilities of the Happy Breathing Machine. The Spiros was only compared to it's average flow rate because the Spiros breathing patterns, both slow and fast, exhibited fairly uniform flow rates, while the Ventodisk breathing patterns exhibited large changes in flow rate. All the flow configurations used within a comparison inhaled the same volume. Table 6.1 summarizes all the flow rates and patterns compared.

Inhaler Used	Flow Pattern Name	Flow rate #1 (liters/min)	Flow rate #2 (liters/min)	Volume (liters)
Ventodisk	Ventodisk Slow Pattern	72 (Avg)	117 (Max)	2.09
Ventodisk	Ventodisk Fast Pattern	165 (Avg)	100 (USP)	3.28
Spiros	Spiros Slow Pattern	12 (Avg)	---	0.80
Spiros	Spiros Slow Pattern	24 (Avg)	---	2.20

Table 6.1. Listing of the flow rates and breathing patterns to be compared in each device including the volume of each set of comparing flows.

The tests completed with each device were very similar to the validation tests. Both of the devices were loaded with salbutamol sulphate powder formulation (with lactose acting as a drug carrier) as supplied by the manufacturer of the device. Each combination of device and sampling flow went through the same set of tests, which consisted of five runs each. A run consisted of collecting three doses of drug from the inhaler device.

6.3. Test Results

The results of the experimental tests are presented graphically in Figures 6.1 to 6.4. Each figure presents the averaged cumulative size distributions of the sampling flows being compared. The vertical bars represent the standard deviation of each impactor stages 5-run averaged data. The results were also compared statistically, to emphasize any significant differences that might exist between the distributions being evaluated. Analysis of variance (ANOVA) was employed to enable comparisons of more than two data sets simultaneously. The statistical analysis consisted of testing the MMADs and GSDs of the five runs for each test set. The logarithms of the MMAD and GSD were used in the analysis. This transformation was done to have data more closely resembling normal distributions in the statistical analysis. Numerical values of MMAD and GSD are given in Table 6.2.

6.3.1. Ventodisk

Figure 6.1 presents the results of the Ventodisk slow pattern test. This test consisted of runs using the Ventodisk slow breathing pattern, its average and it maximum flow rates. As can be seen in Figure 6.1, all three sets of data appear very similar. Statistical analysis confirms that there is no significant difference between any of the MMADs of the

Comparative Test	Flow Pattern Name or Flow rate (liters/min)	Average MMAD (Std. Dev.)	Average GSD (Std. Dev.)
Ventodisk Slow Test	Slow Ventodisk	2.04 (0.17)	1.75 (0.10)
	72 (Avg)	1.92 (0.13)	1.82 (0.11)
	117 (Max)	1.80 (0.09)	1.69 (0.09)
Ventodisk Fast Test	Fast Ventodisk	1.86 (0.09)	1.83 (0.12)
	165 (Avg)	1.75 (0.05)	1.71 (0.11)
	100 (USP)	1.89 (0.11)	1.74 (0.13)
Spiros Slow Test	Slow Spiros	2.07 (0.16)	1.81 (0.09)
	12 (Avg)	2.13 (0.09)	1.84 (0.11)
Spiros Fast Test	Fast Spiros	1.98 (0.13)	1.79 (0.11)
	24 (Avg)	2.17 (0.18)	1.87 (0.29)

Table 6.2 MMADs and GSDs for the 5-run grouped test data.

distributions (ANOVA, $P>0.01$). Additionally, there was no significant difference between the GSDs of any of these data sets (ANOVA, $P>0.01$).

Figure 6.2 presents the results of the Ventodisk fast pattern test. This test consisted of runs using the Ventodisk fast breathing pattern, its average flow rate and the USP flow rate. As shown in Figure 6.2, all three data sets appear quite similar. Again, statistical analysis confirms that no significant difference in any if the MMADs of the distributions exist (ANOVA, $P>0.01$). No significant difference between the GSDs of any of the data sets was determined either (Student's *t*-Test, $P>0.01$).

While the above analysis showed no significant differences in MMAD, differences approaching significant were found for three situations, the slow breath pattern vs. it's peak flow rate of 117 liters/min (Student's *t*-Test, $P=0.021$), the fast breath pattern vs. it's average flow rate of 165 liters/min (Student's *t*-Test, $P=0.038$) and 165 liters/min vs. 100 liters/min (Student's *t*-Test, $P=0.026$). Also of note is that comparing between fast and slow types of breaths showed a significant difference between the slow breath pattern vs. the 165 liter/min flow rate (Student's *t*-Test, $P<0.01$).

It is generally accepted that for inhalers where the aerosol dispersion is powered solely by the patient (such as the Ventodisk), the size distribution of the delivered aerosol is dependent upon the flow rate through the device (e.g. Newman *et al.* (1994)). This theory is also supported by the results of this test when comparing fast vs. slow breaths, however these

results indicate that this flow rate dependence does not translate into significant differences in MMAD when comparing constant flow rates to actual breath patterns that have similar average flow rates. A possible explanation of this can be proposed by looking at particle deaggregation with actual-patient breath patterns. In particular, significant particle uptake does not occur until substantial flow rates have been reached. Particle deaggregation would then occur at the instantaneous flow rate that uptake occurs. This trend is also evident in other devices such as the Rotohaler® (Clark & Bailey (1996)). This tendency of the Ventodisk would cause the aerosols generated with breathing patterns to closely resemble aerosols generated at constant flow rates that resemble breath patterns average flow rates.

These tests indicate that, for the Ventodisk inhaler, a constant flow rate is an acceptable alternative to a realistic breathing pattern, provided the constant flow rate is similar to the patterns average flow rate. They also indicate that the size distribution of the aerosol produced by the Ventodisk is somewhat dependent upon the flow rate or flow pattern through the device, and more importantly, upon the flow rate through the device during powder uptake and deaggregation.

6.3.2. Spiros

Both sets of tests for the Spiros inhaler included only one comparison, i.e. the breathing pattern versus its average flow rate. Figure 6.3 presents the results of the Spiros slow pattern test. Figure 6.3 shows that both data sets appear very similar. Statistical analysis confirms that there is no significant difference between the MMADs or GSDs of the data sets (ANOVA, $P>0.01$).

Figure 6.4 presents the results of the Spiros fast breathing pattern test. Again, both data sets appear quite similar and statistical analysis confirms that no significant difference between the MMADs or GSDs exist (ANOVA, $P>0.01$).

As an additional comparison, the fast and slow breathing pattern data sets and their average flow rate data sets were all compared together. Statistical analysis concludes that there are no significant differences between any of the sets of data obtained from using the Spiros inhaler (ANOVA, $P>0.01$). These findings are also supported by Hill *et al.* (1996) whose clinical studies using gamma scintigraphy found that the Spiros inhaler provided a dose to the lung that was relatively independent of flow rate. These results were not unexpected for the Spiros inhaler since it uses a battery-powered impeller to assist in deaggregating the particles instead of relying totally on the inhalation breath of the patient.

These tests indicate that a constant flow rate is an acceptable alternative to a realistic breathing pattern for the Spiros inhaler. They also indicate that the size distribution of the aerosol produced by the Spiros inhaler is relatively independent of the inhalation flow rate or flow pattern used during actuation of the device.

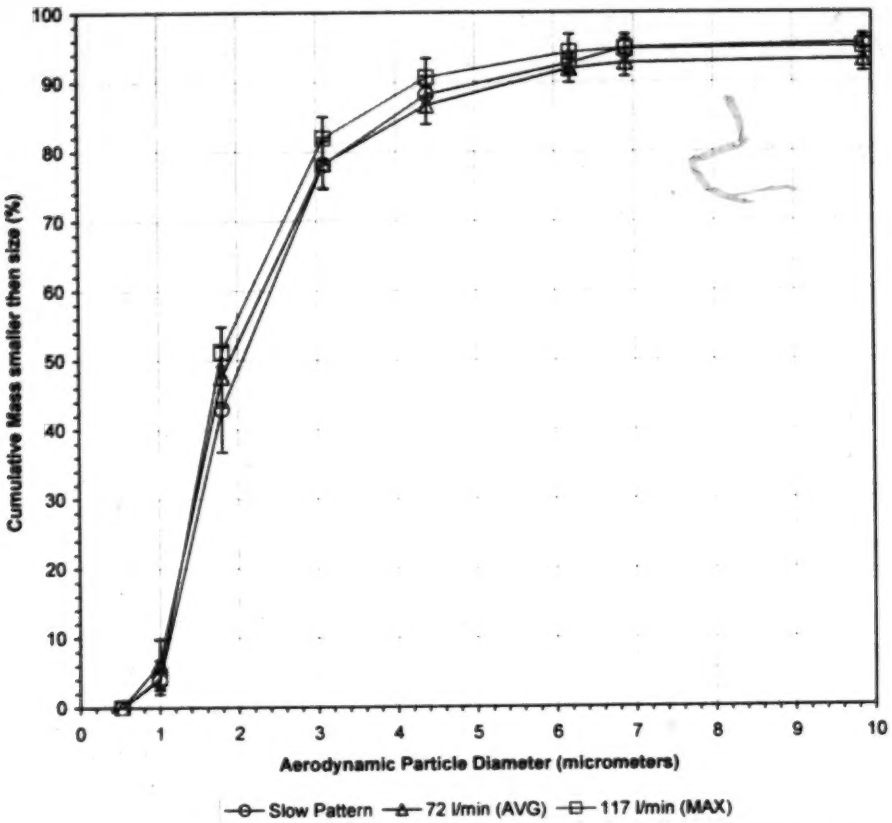

Figure 6.1. Size distributions of the slow breathing pattern tests for the Ventodisk inhaler.

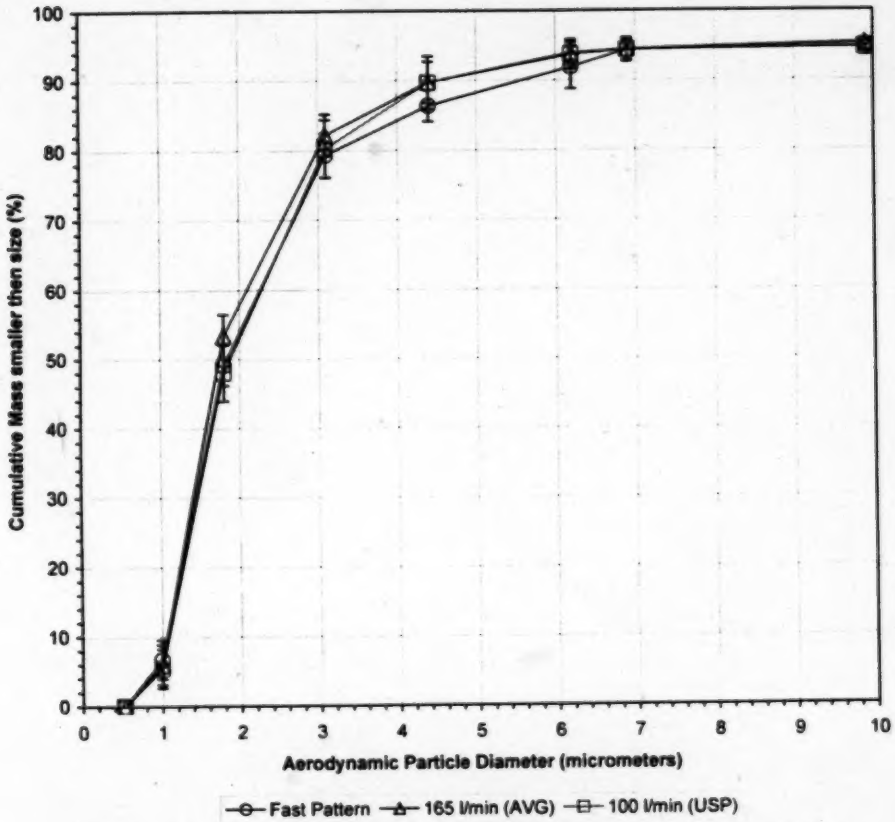

Figure 6.2. Size distributions of the fast breathing pattern tests for the Ventodisk inhaler.

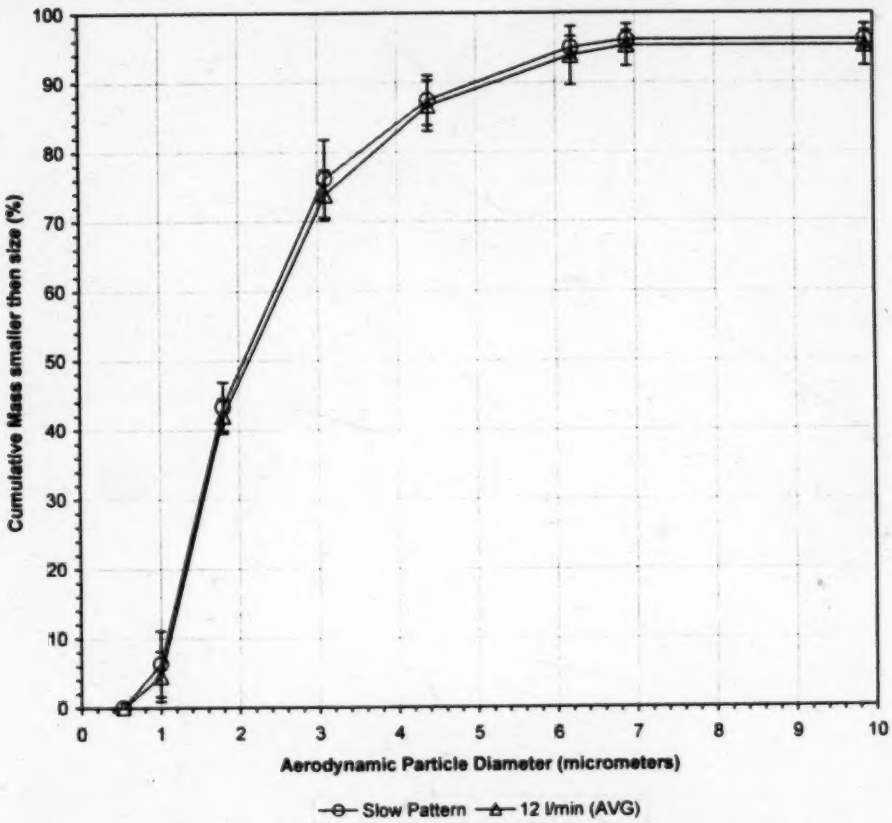

Figure 6.3. Size distributions of the slow breathing pattern tests for the Spiros inhaler.

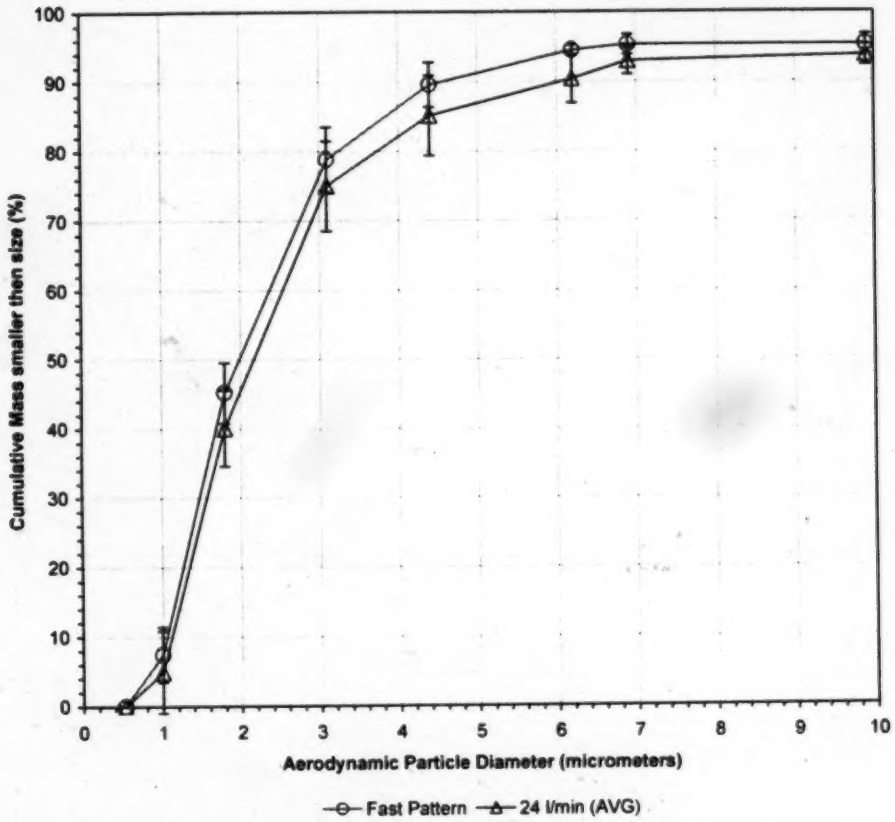

Figure 6.4. Size distributions of the fast breathing pattern tests for the Spiros inhaler.

7. Conclusions and Future Work

This manuscript has presented the work done to investigate the affect of inhalation flow patterns through dry powder inhalers on the aerosol size distribution. A novel device setup was introduced to collect and measure the aerosol using any programmable flow pattern. This device, nicknamed the CAVIC, consisted of a model mouth and throat that closely approximates the actual extrathoracic airways, a breathing simulation machine called The Happy Breathing Machine and a Cascade and Virtual Impactor combination.

Validation of the CAVIC concludes that it works well for aerosols with MMADs smaller than about 2-3μm. This was confirmed experimentally with both the Ventodisk inhaler (Diskhaler inhaler with salbutamol sulphate powder) and the Spiros inhaler (with salbutamol sulphate powder) as neither device suffered significant deaggregation of drug particles or excessive collection losses. CAVIC validation also concludes that aerosols with MMADs larger than about 3μm could be susceptible to particle deaggregation and excessive collection losses. This was confirmed experimentally with the Bricanyl Turbuhaler (with terbutaline sulphate powder) as collection losses were excessive and the MMAD was not measured accurately.

Future work would naturally consist of further validation with different inhaler and drug powder combinations to better characterize the useful limits of the CAVIC. Investigation into the specific cause of malfunction of the CAVIC with the Turbuhaler (i.e. particle deaggregation, collection loss or both etc.) would also be of great benefit.

This manuscript concludes that the effect of flow pattern on aerosol size distribution varies between devices and drugs used. The two devices tested demonstrated similar effects of flow rate and flow pattern on the size distribution of the produced aerosol. While the Spiros inhaler showed no significant changes to the aerosol size distribution regardless of the flow rate or flow pattern used, the Ventodisk inhaler did show some changes to the size

distributions of the produced aerosols. These results indicate that *in vitro* testing of the Spiros or Ventodisk inhalers with constant flow rates is acceptable, provided the flow rate used resembles the average flow rate expected during actual patient use. This offers an important finding since it provides support for the use of constant flow rate *in vitro* testing, which is much simpler.

This work naturally extends to testing of additional inhaler and drug combinations, just as with the validation. Various other breathing patterns and flow rates could also be tested in the future to extend the conclusions of this work to higher and lower flow rates.

8. References

Clark A.R., Bailey R. (1996). Inspiratory Flow Profiles in Disease and Their Effects on the Delivery Characteristics of Dry Powder Inhalers. *Respiratory Drug Delivery Program and Proceedings.* Dalby R.N., Byron P.R., Farr S.J., eds. Interpharm Press, Buffalo Grove, Illinois. p.221-230.

French D.L., Edwards D.A., Niven R.W. (1996). The influence of formulation on emission, deaggregation and deposition of dry powders for inhalation. *Journal of Aerosol Science.* **27(5)**: 769-783.

Hill M., Vaughan L., Dolovich M. (1996). Dose Targetting for Dry Powder Inhalers. *Respiratory Drug Delivery Program and Proceedings.* Dalby R.N., Byron P.R., Farr S.J., eds. Interpharm Press, Buffalo Grove, Illinois. p.197-208.

Israelachvili J. (1992). *Intermolecular and Surface Forces*, Academic Press, New York.

Newman S.P., Hollingsworth A., Clark A.R. (1994). Effect of Different Modes of Inhalation on Drug Delivery from Dry Powder Inhalers. *International Journal of Pharmaceuticals.* **102**: 127-132.

Tennekes H., Lumley J.L. (1972) *A first course in turbulence*, MIT Press, Cambridge, Mass.

White F.M. (1974). *Viscous fluid flow*, McGraw Hill, New York.

Willeke K., Baron P.A. (1993) *Aerosol Measurement*, Van Nostrand Reinhold, New York.